

# Evaluation of an in situ QAM-based Power Line Communication system for lithium-ion batteries

Mahyar J. Koshkouei  | Erik Kampert  | Andrew D. Moore | Matthew D. Higgins

WMG, University of Warwick, Coventry, UK

## Correspondence

Mahyar J. Koshkouei, WMG, University of Warwick, Coventry, CV4 7AL, UK.  
Email: [mahyar.koshkouei@warwick.ac.uk](mailto:mahyar.koshkouei@warwick.ac.uk)

## Funding information

Engineering and Physical Sciences Research Council, Grant/Award Numbers: EP/N509796/1, EP/R513374/1

## Abstract

Power Line Communication (PLC) is used to transmit high-fidelity data on internal cell characteristics from within instrumented cells to an external Battery Management System (BMS). Using PLC is beneficial, as it avoids the need for a complex and heavyweight wiring harness within a battery. The use of advanced modulation, such as Quadrature Amplitude Modulation (QAM), is considered here. The existing experimental results of lithium-ion cell impedance characteristics for frequencies of 100 kHz–200 MHz are exploited in order to create a realistic battery model. This model is used to determine the effectiveness and optimal properties of PLC with QAM, as a means of in situ battery communication for Battery Electric Vehicles (BEVs) in combination with a real-world dynamic drive profile. Simulations reveal that the performance of the PLC system is heavily dependent on the selected carrier frequency due to the significant changes in reactance and internal resistance of the lithium-ion cells tested. Furthermore, cells placed in parallel display a decreased performance compared with cells in series. The results highlight that the optimal carrier frequency for in situ QAM-based PLC for a lithium-ion battery system is 30 MHz, and that additional signal conditioning is required for 4-QAM and higher modulation orders.

## 1 | INTRODUCTION

Battery Electric Vehicles (BEVs) offer significant advantages over traditional Internal Combustion Engine Vehicles (ICEVs), including lower toxic gas emissions, higher energy, and lower running costs which in turn improve accessibility [1–4]. However, BEVs currently also have significant disadvantages that hinder their popularity within the global light-vehicle market share, which include the relatively low energy density of energy storage systems, limited driving range on a single charge, long charging time, and perceived comparative high purchase and running costs [5–8]. Hence, new technologies and techniques are necessary to tackle these limitations.

Energy storage systems consisting of many individual lithium-ion (Li-ion) cells are typically used within BEVs, thanks to their high capacity, energy density, power density, and lack of memory effects in comparison to other battery chemistries, such as nickel-metal hydride and lead acid [9]. Nevertheless, a Li-ion cell is sensitive to a variety of factors, such as ambient and internal temperatures, working voltages, and charge/

discharge current rates. Operating a Li-ion cell outside of its small safety window will shorten its lifetime and performance, and further abuse may cause thermal runaway, fire, or even explosion [10–12].

The use of the Battery Management System (BMS) is therefore the best practice for monitoring the status and mitigating any failure of Li-ion cells within a typical BEV battery pack. The BMS estimates the state of charge (SoC) and state of health (SoH) of the connected Li-ion cells within a battery pack, and uses this estimation to perform actions such as cell charge balancing, to mitigate overcharging and deep discharging; accelerated ageing; and permanent damage [13–15]. Many methods have been studied for the estimation of the SoC and SoH, including extended Kalman filter techniques [16, 17], such as the splice Kalman filter algorithm [18].

The effectiveness of the BMS on the SoH of Li-ion cells may be increased by improving the quality and quantity of cell characteristic data available at run-time. This may be through the use of thermo-electrochemical instrumentation of the cell [19]. Using this additional information, the BMS could then recognise

This is an open access article under the terms of the Creative Commons Attribution License, which permits use, distribution and reproduction in any medium, provided the original work is properly cited.

© 2021 The Authors. *IET Electrical Systems in Transportation* published by John Wiley & Sons Ltd on behalf of The Institution of Engineering and Technology.

the various tolerances of the cells within the pack, and use that knowledge to apply enhanced real-time coordination features to specific cells, such as self-reconfiguration [20] and temperature regulation [21]. This intelligence improves performance by taking advantage of cells that are highly tolerant of harsh environments, and improving safety without abusing cells that have lower tolerances.

To collect this particular cell characteristic data, a communication system is required to allow for the data transfer between the cells within the battery pack and the BMS. Power Line Communication (PLC) is the best approach for in situ battery pack communication, thanks to the lack of requiring any additional wire harness that increases the complexity and weight of the energy storage system [22, 23]. However, the in situ characteristics of a typical BEV battery pack must be evaluated for its usability as a transmission medium. This includes determining the characteristics for Li-ion cells in various configurations, including different combinations of cells placed in series and parallel that are commonly used within BEVs. In addition, the possibility of utilising advanced modulation techniques such as Quadrature Amplitude Modulation (QAM), which makes more efficient use of the communication channel, requires further study. Whereas higher modulation orders of QAM allow for higher data transfer rates, the sensitivity to noise also increases. The BEV battery pack is known to be a harsh environment due to significant noise on the transmission medium, mainly caused by switching regulators [24, 25], so further study is required to measure the effect of this noise on a QAM PLC system.

In this paper, previously published Electrochemical Impedance Spectroscopy (EIS) measurements of both two Li-ion cells in series [26], as well as two cells in parallel [27] are used to create a new battery model that is utilised to verify the performance of PLC within a typical BEV battery pack. This paper also considers the effects on the performance of PLC using QAM for Li-ion cells positioned in parallel and series, and the impact of noise on the transmission medium.

The key contributions of this work are as follows:

1. Analysis of Li-ion cells as a communication medium for PLC with QAM, for signal carrier frequencies between 100 kHz and 200 MHz.
2. A comparison of prospective signal carrier frequencies based upon their capability to reduce the impact of any noise during operation.
3. Recommendations of carrier frequency and QAM modulation order for prospective PLC systems within Li-ion energy storage systems based upon the obtained results from the proposed method in this paper.

This paper is organised as follows: Section 2 provides a brief literature review on the existing in situ BEV battery pack PLC systems and their limitations; Section 3 addresses the methodology utilised to create and use the BEV energy storage system model; Sections 4 and 5 present the results and conclusions, respectively.

## 2 | SYSTEM DESCRIPTION

The existing techniques demonstrate the use of high frequency PLC through Li-ion cells, but these methods are limited in their design and functionality. A circuit-based model of 13 Li-ion prismatic cells in series for the frequency range of 1 kHz–100 MHz has been demonstrated in [24]. In their work, it has been claimed that the proposed circuit-based model can be used to simulate the channel characteristics of a Li-ion battery with more cells than those used to create the model. However, further research is required into the modelling of other types of Li-ion cells, including pouch and cylindrical, which are also commonly used within automotive energy storage systems.

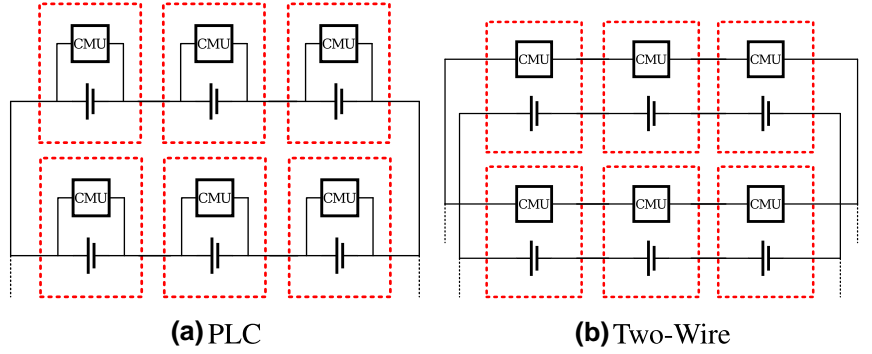
A structure of a BMS using a separate two-wire communication bus in a tiered system of cell management units, module management units, and a pack management unit has been designed in [28]. This system proved to deliver a data rate of 100 kbps using On–Off Keying (OOK) modulation. However, a wire harness was needed due to the independent communication bus used, in contrast to a system utilising PLC as proposed in this paper. By using time slicing to share the communication bus, only two additional wires were required for each set of cells in series, as opposed to using two separate wires for each cell in the battery pack. Despite this fact, the need for any wiring harness still increased the complexity and weight of the energy storage system as shown in Figure 1. In this paper, a PLC system is proposed which does not need any wiring harness and therefore mitigates complications associated with unnecessary additional weight. Furthermore, by utilising QAM as opposed to OOK, higher data rates can be achieved.

Recent work characterised the impedance of six 18650 Li-ion cells in series, and has demonstrated battery PLC with a carrier frequency of 20 MHz [29]. The transfer of data using asynchronous serial communication with OOK produced no errors. Further research is required to determine the effects of Li-ion cells in a configuration of both series and parallel arrays. In addition, the Li-ion cells used were of proprietary technology, which makes it unclear as to whether other Li-ion types, such as a lithium nickel manganese cobalt oxide (NMC) 18650 cell [30], were analogous to the cells tested.

A PLC system that utilised the Controller Area Network (CAN) bus was designed in [31]. The CAN bus is an existing vehicle bus standard that is widely available as a peripheral within microcontrollers. The use of CAN as opposed to a bespoke communication bus was therefore advantageous as it allowed for easier integration within existing systems. However, the system was only suitable for small scale PLC networks, and a current limitation was imposed due to the use of choke inductors. These problems must be solved before the use of this system can be realised within a BEV due to the potentially large number of networked cells within the battery, and the high power output required to drive the vehicle.

The basis of an in situ PLC system for a small configuration of instrumented cylindrical 21700 Li-ion cells has been

**FIGURE 1** Schematic comparison between PLC and two-wire communication architectures for energy storage systems. PLC, Power Line Communication



designed and demonstrated in [32]. The system was verified using various tests, including controlled current experiments. It achieved a low BER of 0.002% and an average response time of 45.6 ms when using an existing PLC integrated circuit configured for 56 kbps serial communication at 6 MHz. Further work is required to improve the communication performance of this system; the data rate must be improved in order to accommodate the large number of networked cells within a typical BEV battery.

This paper improves the communication performance by using experimental data of Li-ion cell characteristics to examine carrier frequencies of up to 200 MHz. In addition, the use of QAM is simulated for its effectiveness in allowing for an increase in data communication rate without changing the carrier frequency. As already stated, the existing methods of electrochemical cell communication have significant limitations and disadvantages. To overcome these limitations, this paper considers a QAM signal across NMC 18650 cylindrical cells in series and parallel. QAM utilises both amplitude shift keying (ASK) and phase shift keying (PSK) in order to represent data using a constellation matrix. QAM offers a more efficient occupation of the transmission channel compared with ASK and PSK, which leads to a higher transmission rate given the same bit error rate (BER) [33]. However, the modulation order of QAM is limited by the signal-to-noise ratio (SNR), which must be greater than a certain threshold for the decoder to distinguish between QAM symbols.

### 3 | EXPERIMENTAL DETAILS

The EIS of Li-ion cells is used to estimate various characteristics useful for degradation mitigation. This includes prediction of SoH and SoC by performing an EIS measurement, which pulses a Li-ion cell at low frequencies of typically 10 mHz–5 kHz, in order to determine the cell's impedance [34]. To achieve an appropriate symbol rate of at least 100 kbps in a prospective communication system, it is expected that the carrier frequency is at least 2 orders of magnitudes higher than that used in typical EIS applications. This paper, therefore, considers carrier frequencies between 100 kHz and 200 MHz to determine the best obtainable parameters possible for an in situ Li-ion energy storage PLC system with respect to given symbol rates and noise rejection performance.

Using EIS, impedance measurements of individual Li-ion cells are obtained. Electrical impedance possesses both a phase and a magnitude that can be obtained from reactance and resistance measurements, respectively. The reactance of a Li-ion cell affects the phase shift or delay of the signal transmitted through it. If the phase shift between current and voltage is positive, then the circuit shows inductive behaviour, whereas if it is negative, the circuit shows capacitive behaviour. The internal resistance of the cell forms a potential divider with the circuit it is connected to, and therefore affects the attenuation of the transmitted signal; as the internal resistance increases, the output voltage decreases. Hence, the potential difference of the electrochemical cell must be known before its internal resistance can be determined. The load of the circuit in this instance varies due to the use of the BEV through driving [35]. The attenuation of the transmitted signal may change at any time, and thus must be taken into account by the communication system.

Various methods exist for performing EIS at high frequencies in order to obtain the impedance of a circuit or component. This includes using a potentiostat or galvanostat, whereby the voltage or current is kept constant, respectively. This paper uses real experimental data presented in [26, 27] to design a novel battery model used to determine the impedance and phase for two 18650 Li-ion cells in series, and also in parallel, for signals modulated between 100 kHz and 200 MHz. The designed battery model will then be used to simulate the effects of the Li-ion cells on the PLC signals transmitted in order to determine optimal parameters for the proposed PLC system.

An electrical impedance contains a real and an imaginary component in the form of resistance  $R$  and reactance  $X$ . By using the impedance and phase measurement data from the EIS, first, the reactance  $X$  is calculated using the impedance  $Z$  and the phase  $\phi$  between  $Z$  and  $R$ :

$$X = Z \sin \phi \quad (1)$$

Then, the internal cell resistance  $R$  is calculated from the impedance and reactance:

$$R = \sqrt{Z^2 - X^2} \quad (2)$$

By performing these calculations on the existing data, the expected attenuation applied to the signal transmitted through

the Li-ion cell is determined. In this paper, it is first assumed that the load connected to the Li-ion cell is  $1 \Omega$ . A second simulation is performed using load profile data obtained from real driving of a vehicle on a motorway [35]. These simulations are used to determine the effects of the Li-ion cells, and user driving on the communication system, respectively.

So far, only the effects of the Li-ion cells on PLC systems have been considered. It is also required to consider the effects of expected noise within the target communication medium. The maximum noise level expected within a BEV energy storage system must be applied to the transmitted signal to improve the accuracy of the system model. The most significant noise has been shown to be produced by the DC–DC converter within powertrain systems, which causes spikes of up to 2 MHz noise. An additional 12 MHz noise can be caused by the operation of the CAN signal bus [36].

A process diagram of the used methodology for the series of tests presented in this paper is shown in Figure 2, and a summary of the experimental parameters and values described within this section is presented in Table 1.  $10^7$  QAM symbols of random data are modulated in orders of 2, 4, 8, 16, 32, 64, 128, and 256. Each QAM signal is then processed by the simulated energy storage system model, by first applying the calculated delay and gain for the battery configuration under test. Thereafter, the load is taken into account, either as a static  $1 \Omega$  load or taken from the dynamic drive profile. For the latter scenario, the actual transmission times of each of the  $10^7$  QAM symbols are used, and the simulated load is adjusted to the dynamic load at that specific time. Finally, the noise that is expected within the target transmission medium is added. After transmitting the QAM signal through the simulated energy storage system model, the resultant signal is demodulated to obtain a binary data stream that is then compared with the original transmitted data. The BER is calculated by comparing each bit of the two data streams, and the symbol error rate (SER) compares the symbols that the bits represent. Hence, SER is more sensitive to errors in data, and is always equal to or higher than BER. An in-depth investigation of the type and extent of signal conditioning required to reduce the BER and SER falls outside the scope of this analysis.

**TABLE 1** Parameters and their value ranges as used in the experimental method

Parameter	Value
Battery load	Static $1 \Omega$ or Dynamic Drive
QAM modulation order	2, 4, 8, 16, 32, 64, 128, 256
Number of symbols	$10^7$
Carrier frequency	100 kHz–200 MHz
Frequency step	100 kHz
Li-ion cell configuration	Two in parallel or in series
Drive profile ambient temperature	$10^\circ\text{C}$

## 4 | RESULTS AND DISCUSSION

This section presents the results obtained using the methodology described in Section 3, and evaluates the usability of the PLC systems under test. Furthermore, various parameters including carrier frequencies and battery configuration of a prospective PLC system for in situ lithium-ion energy storage systems are discussed.

The Nyquist plots shown in Figure 3 of two Li-ion cells in series and parallel are used to determine the phase angle and the internal resistance of the cells. The difference in resistance  $R$  and reactance  $X$  between both configurations shown can already be observed, whereby the parallel configuration shown in Figure 3a shows much greater inductive reactance, capacitive reactance, and resistance in comparison to the series configuration illustrated in Figure 3b. Moreover, it can be seen that a large change in both resistance and reactance occurs across the small frequency range of 90–130 MHz for cells tested in parallel configuration. In fact, the resistance  $R$  reaches a peak of  $374 \Omega$  near 110 MHz, and the reactance  $X$  varies between  $196 X_L$  and  $155 X_C$ . In contrast, cells in series configuration exhibit a gradual change in resistance and reactance for all carrier frequencies tested, reaching a peak resistance of  $19 \Omega$  near 150 MHz, and reactances of up to  $12.5 X_L$  and  $3.1 X_C$ .

Figure 4 presents the magnitude of the phase change and attenuation of PLC signals transmitted through Li-ion cells. A direct comparison of Figure 4a,b indicates that two Li-ion cells in series have a more negative impact in terms of attenuation across the spectrum of carrier frequencies tested. For the parallel configuration as shown in Figure 4a, the two Li-ion cells display the largest attenuation with a near-zero gain at a carrier frequency of 110 MHz, before recovering towards a gain of 1 at 200 MHz. On the other hand, for the series configuration as shown in Figure 4b, the gain falls slowly to 0.05 at 153 MHz, and then only rises slowly towards a gain of 0.15 at 200 MHz. Whereas a parallel cell arrangement results in a stable gain of 0.7 between 13 and 40 MHz, for a series configuration, the lower the carrier frequency, the less attenuation is observed on the signal.

The phase shift of the signal transmitted through two Li-ion cells in parallel, as shown in Figure 4a, is significant throughout the carrier frequencies tested, nearing both  $-90^\circ$  and  $90^\circ$  for most of the carrier frequencies tested. However, at 110 MHz, the phase delay crosses  $0^\circ$  as it quickly deviates from  $90^\circ$  to  $-90^\circ$ . The effect of this momentary lack of delay at 110 MHz is shown in the following analysis, whereby an improvement in error rates is seen for all QAM symbol rates. Nevertheless, the attenuation at 110 MHz is too large for this carrier frequency to be useful, unless significant signal conditioning is added for every two Li-ion cells in parallel to compensate for the signal loss. It is possible that even small changes in characteristics of the Li-ion cell could significantly alter the phase shift of the transmitted signal, due to the sharp change in phase with frequency. However, the phase shift of two cells in series, as shown in Figure 4b, does not fluctuate as significantly, reaching a maximum of  $66^\circ$ , before a trough that

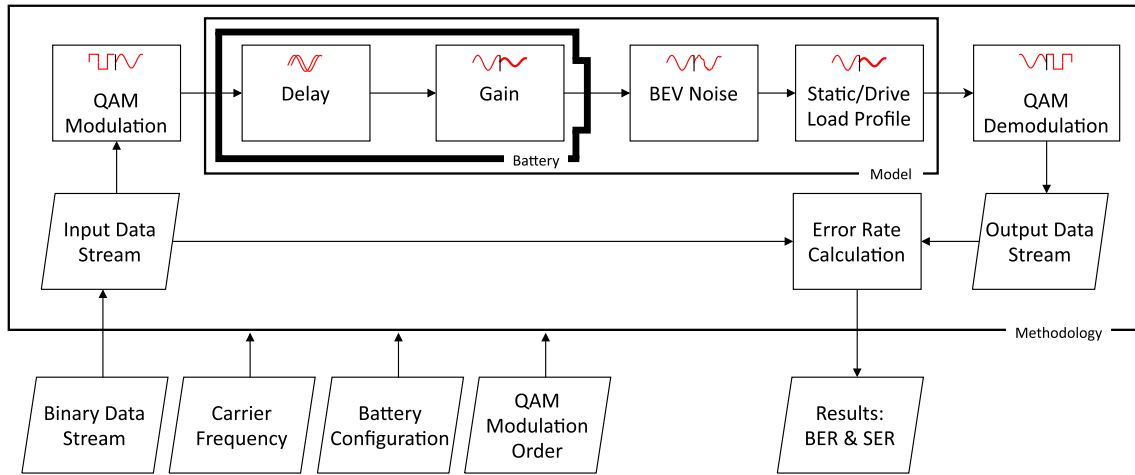


FIGURE 2 Process diagram of the experimental method

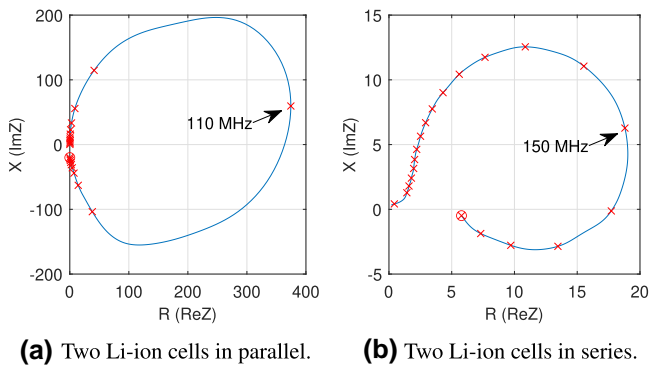


FIGURE 3 Nyquist plots of two Li-ion cells in parallel and in series. Circle and cross markers indicate steps of 200 and 10 MHz, respectively. The marker for the largest resistance is labelled

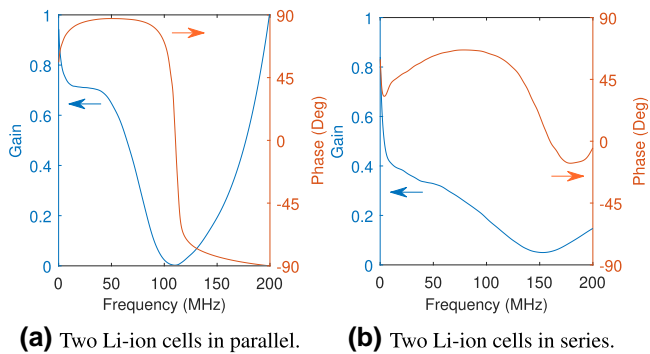


FIGURE 4 The carrier frequency dependence of the phase and gain of PLC signals transmitted through two Li-ion cells

falls to a minimum of  $-16^\circ$ . If both parallel and series configurations are then taken into account, the performance of the PLC system is expected to be optimal at 30 MHz, where both the attenuation and the phase remain to be most steady. At this frequency, the communication system is thus less susceptible to clock jitter noise, and may therefore use wider communication channels.

Figure 5a,b shows the BER and SER of data streams transmitted with PLC using various QAM orders through a model representing two Li-ion cells in series, respectively. It can be observed that both BER and SER are either low at  $10^{-7}$ , or tend to 1 due to the majority of data transmitted becoming corrupt. By comparing both figures, it can be shown that 2-QAM is not affected by the characteristics of the Li-ion cells throughout the entire frequency spectrum tested. In comparison, of the other modulation orders, only 4-QAM signals are able to approach a BER and SER of  $10^{-7}$  at frequencies of 1–14 MHz, and 134–200 MHz. Modulation orders higher than 4-QAM fail to demonstrate any reasonable data communication.

Figure 5c,d display the BER and SER of data streams transmitted through the battery model representing two Li-ion cells in parallel, respectively. When they are compared with the data transmission through two cells in series, these results show degraded performance. Moreover, the results indicate that 2-QAM is able to keep a BER and SER of  $10^{-7}$  between 100 kHz and 199 MHz, but then immediately increases to a maximum SER of 1 at 200 MHz. Of the other higher order modulated data streams, only 4-QAM is able to demonstrate stability at any point across the tested frequencies. Between 106 and 114 MHz, the data stream modulated with 4-QAM yields a BER and SER of  $10^{-7}$ , deviating from a SER of 1 presented at all other carrier frequencies tested. In fact, at these frequencies, all other QAM orders show a decrease in both BER and SER. For instance, the BER and SER of 8-QAM at 110.6 MHz are reduced to 0.16 and 0.48, from the maximum of 0.49 and 1, respectively. This improvement in error rate is reduced with increasing QAM order. As already stated, this sudden improvement in BER and SER occurs within the same range of frequencies that produces a significant change in resistance and reactance within the Nyquist plot shown in Figure 3a.

From these results, it can be concluded that using QAM causes increasing error rates with increasing modulation order. Across the carrier frequencies tested, 2-QAM demonstrates the best possible BER and SER for both series and parallel

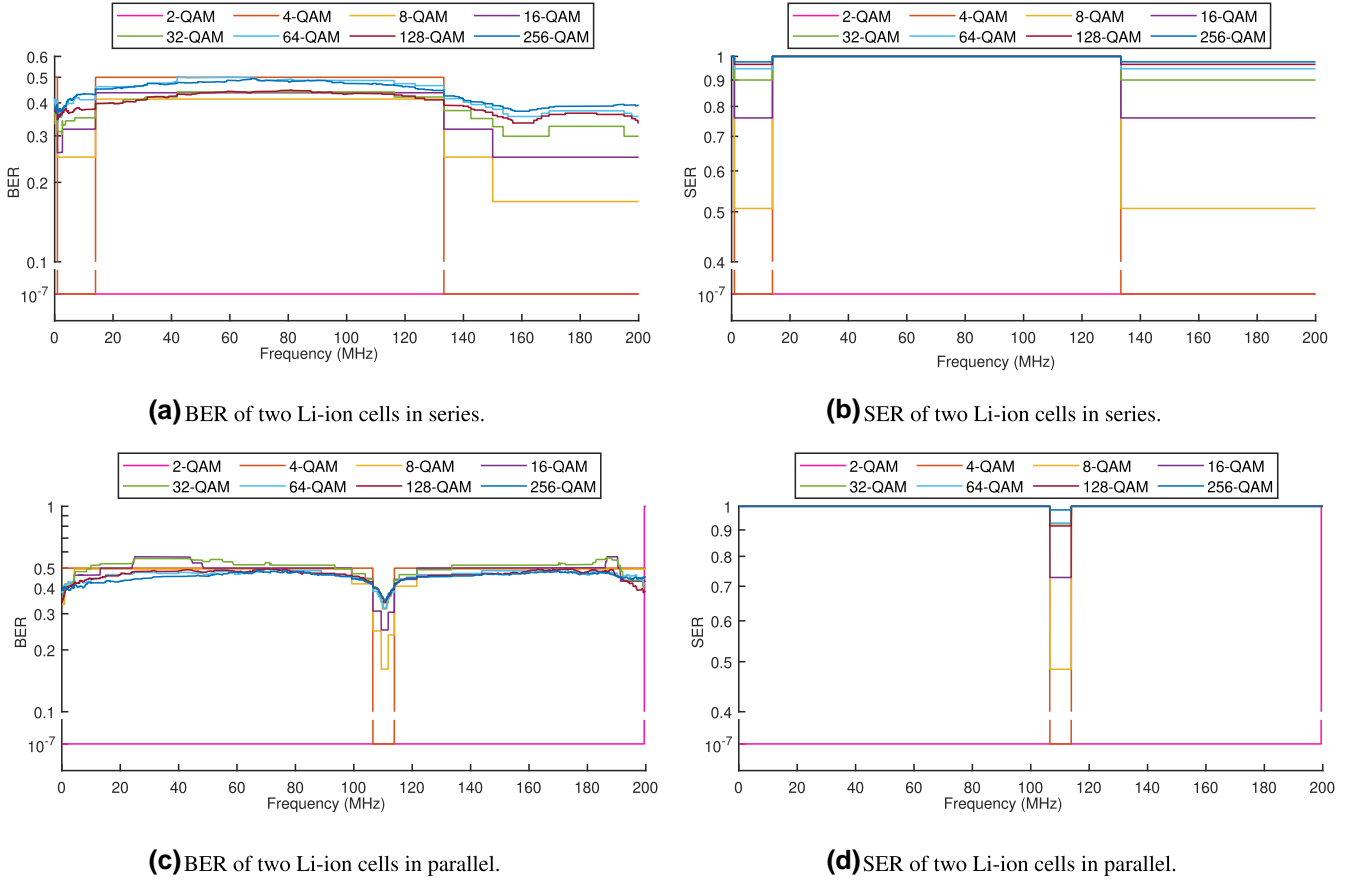


**FIGURE 5** Bit and symbol error rates (BER and SER) of Power Line Communication through Li-ion cells under static  $1 \Omega$  load. QAM, Quadrature Amplitude Modulation

arrangements of the two Li-ion cells modelled. For higher modulation orders of QAM, the window of usable carrier frequencies not only decreases, but varies significantly between series and parallel cell arrangements, whereby the parallel arrangement poses a much smaller window of 106–114 MHz in comparison to the two windows of 950 kHz–14 MHz and 133–200 MHz for the series arrangement.

Both the BER and SER for serial and parallel configurations displayed no difference between simulations that include expected noise on the target communication channel, such as from switch-mode converters [36], and simulations without noise consideration. By taking into account the intensity of attenuation and phase for specific carrier frequencies and configurations, these results may be used to predict the usability of PLC within a target environment when a noise characterisation for the specific energy storage system is also considered. Due to the wide variety of powertrain systems, it is expected that each of them will have different properties of electromagnetic noise, and therefore should only consider noise for each specific system. Furthermore, consideration must be given to the noise generated as a consequence of user behaviour, such as when acceleration or braking is applied, that may produce spikes of noise large enough to disrupt the communication channel.

The effects of delay and attenuation that the Li-ion cell imposes on the in situ transmitted signal increases with QAM order. As stated in Section 2, QAM uses both PSK and ASK modulation, and the effects of delay and attenuation of the Li-ion cells have a direct influence on the quality of data transmission. The most successful modulation order, 2-QAM, is also known as binary phase shift keying (BPSK) as the only two symbols in the constellation are two states of phase shift and hence does not need any amplitude modulation used in higher orders of QAM. In order to fully exploit the performance benefits of QAM for PLC in terms of achievable data rates, at least 4-QAM must be used.

Through focussing on the resultant QAM constellation plots for each modulation order, it can be observed why the error rates are so polarised. For example, Figure 6 visualises that despite both 2-QAM and 4-QAM demonstrating very low error rates, the attenuation is so significant that it is difficult to observe the different constellation points in each plot without significantly reducing axes limits. If such a system is to scale up to many Li-ion cells in parallel, then the use of 110 MHz as a carrier frequency will be unacceptable due to the level of signal amplification required throughout the transmission medium. Therefore, in this case, the smallest amount of noise could cause data corruption. In fact, a carrier frequency of 110 MHz

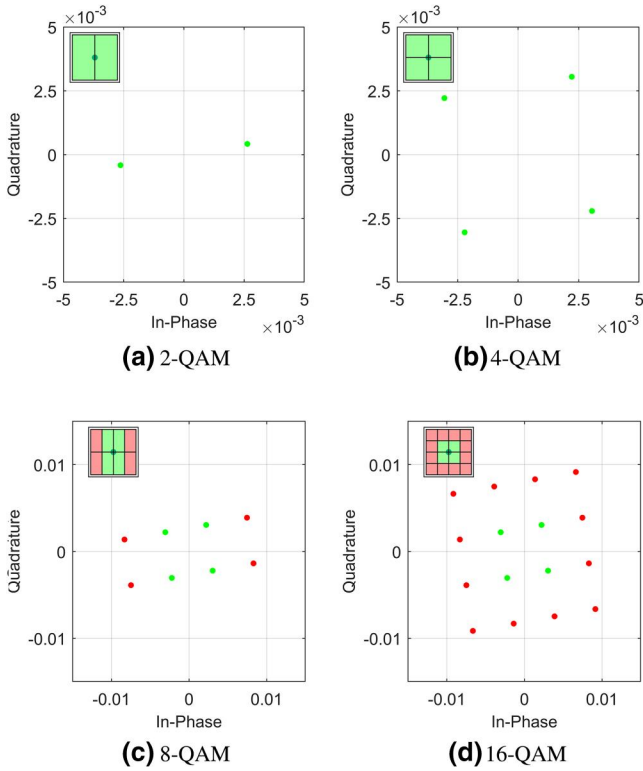


**FIGURE 6** QAM constellations of Power Line Communication data transferred through two Li-ion cells in parallel at carrier frequencies of 110 MHz. Insets show green and red shaded segments that denote constellation points within their correct and incorrect sectors, respectively. QAM, Quadrature Amplitude Modulation

is shown to produce most appropriate results for two Li-ion cells in parallel only because the phase shift is  $\sim 9^\circ$ , which is sufficiently low enough for the QAM symbols to remain within their constellation sector. This response can be observed in Figure 6, whereby the attenuation is so significant that the points approach the origin, yet are still decoded correctly as the constellation points are within their correct sector. However, as the QAM order is increased, symbols that are not mapped to the sectors closest to the origin become invalid due to the significant attenuation that displaces these symbols out of their correct sector. This behaviour can be seen for 8-QAM and 16-QAM, whereby the outer 4 and 12 constellation points are not mapped to their correct sector, respectively. In other words, with increasing QAM order, the system is more prone to attenuation.

Figure 7 illustrates that the magnitude of the 4-QAM signal decreases as the carrier frequency increases from 50 MHz towards 110 MHz. The rate with which the magnitude decreases is greater when the two Li-ion cells are connected in parallel. In fact, Figure 7a shows that there is a decrease in magnitude of 0.68 V between 50 and 110 MHz for a parallel configuration, whereas Figure 7b shows only a decrease in magnitude of 0.25 V for a series configuration. However, Figure 7a shows that whilst the magnitude may be the lowest at 3.8 mV when using a carrier frequency of 110 MHz, the change in phase pushes the constellation points (shown in green) into their correct sectors.

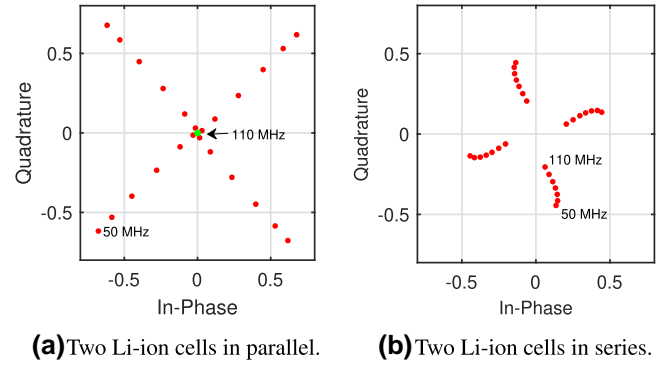


**FIGURE 7** Frequency sweep of 50 to 110 MHz in 10 MHz steps of a 4-QAM signal. The closer the symbol is to the origin, the more significant the attenuation. Green and red markers denote constellation points within their correct and incorrect sectors, respectively. QAM, Quadrature Amplitude Modulation

This change in phase may also be seen in Figure 4a whereby it rapidly decreases towards  $0^\circ$  at 110 MHz. This behaviour corresponds to the improvement in SER that is also observed within Figure 5d. Nevertheless, as already discussed, the high attenuation at 110 MHz means that an increase in the magnitude of noise on the communication channel has the potential to reduce the reliability of the PLC system.

On the other hand, Figure 7b shows that there is only a gradual change in phase and attenuation between 50 and 110 MHz. In fact, over the full range of carrier frequencies tested, the arrangement of two Li-ion cells in series showed only gradual changes in reactance and internal resistance, in comparison to the sharp changes in parallel configuration. This gradual change in phase is not significant enough to push any of the constellation points into their correct sectors at 110 MHz, but rather does so from 133 MHz upwards. However, the attenuation identified in the series configuration does not increase as significantly as seen in the parallel configuration for the same range of carrier frequencies. This performance indicates that less signal conditioning is required for Li-ion cells arranged in series than for cells arranged in parallel. However, phase shift compensation will still be required for both arrangements in order to place QAM symbols within their correct sector.

It is shown in Figure 8 that an improvement in SER can also be seen for PLC transmission through two Li-ion cells in a series configuration when the carrier frequency is increased from 130 to 140 MHz. This improvement is reflected in the reduction in SER for 4-QAM at 140 MHz, as displayed in Figure 5b. The phase shift is too small to cause errors within the data stream as shown by the green points. Despite this, the transmitted QAM symbols are displaced to near the origin, highlighting that the attenuation is so substantial that significant signal conditioning is required in order to achieve an SNR that allows for adequate data transmission rates.

Depending on the carrier frequency selected for the PLC system and the magnitude of the noise on the target transmission channel, signal conditioning techniques may be required. These techniques may consist of automatic gain

control (AGC), phase compensation, and band-pass filters. However, signal-conditioning techniques may be limited by the available space within a BEV battery, and by the reluctance to reduce the energy density of the battery, especially if a significant number of in situ signal conditioning systems are required. Moreover, these signal conditioning techniques may vary between different energy storage systems due to their

unique design, electrochemical chemistry, transmission channel characteristics and cell arrangement.

These results show that the phase shift caused by the Li-ion cell on the transmitted PLC signal varies with frequency. These changes in phase shift are typically significant enough to cause QAM symbols to be displaced from their correct sector, resulting in polarised changes in the achieved BER and SER. Phase shift correction must therefore be utilised to reverse the Li-ion cells' effects of such delay on the signals. Should simultaneous data transfer using frequency division multiple access (FDMA) be required, the significant change in phase shift at 110 MHz will severely hinder the performance of the phase modulation component of QAM, and therefore the communication system. A carrier frequency of 30 MHz is therefore recommended for use within a PLC system utilised within a large BEV Li-ion battery using QAM, on the precondition that phase shift compensation is employed. The required amount of signal conditioning is dependent upon the number of cells arranged in parallel and series within the battery.

Real battery load profile data obtained from a vehicle driving on a motorway near Coventry, United Kingdom [35], is used to determine the effects of dynamic load on the performance of the prospective PLC systems considered. This drive load profile was recorded at an ambient temperature of 10°C for a drive duration of ~44 min. Due to the high carrier

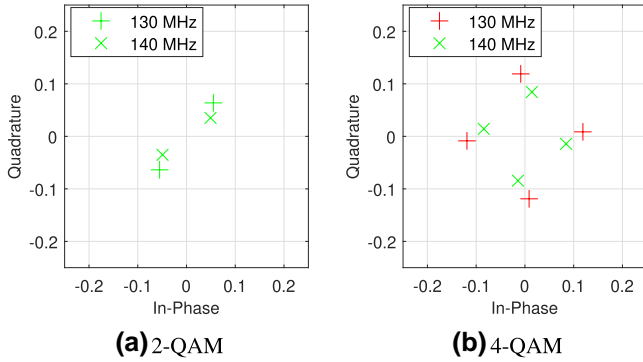


**FIGURE 8** QAM constellations of Power Line Communication data transfer through two Li-ion cells in series at carrier frequencies of 130 and 140 MHz. Green and red markers denote constellation points within their correct and incorrect sectors, respectively. QAM, Quadrature Amplitude Modulation

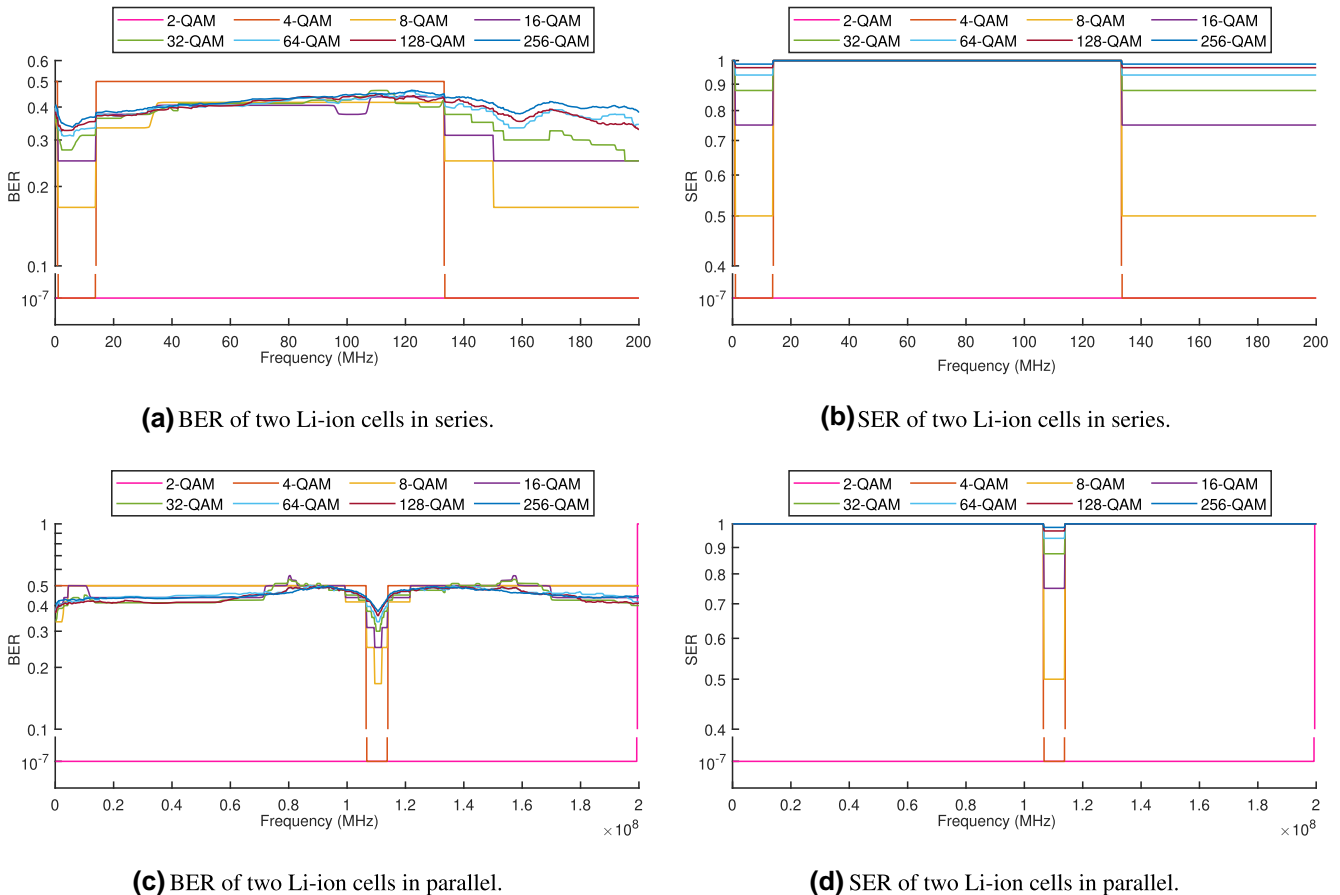


**FIGURE 9** Bit and symbol error rates (BER and SER) of Power Line Communication through Li-ion cells under dynamic drive profile load

frequencies of the communication system under consideration, all of the  $10^7$  symbols are transmitted within 100 s and only 50 ms for carrier frequencies of 100 kHz and 200 MHz, respectively. It is therefore expected that the drive load profile will have less influence on error rates for communication systems utilising higher carrier frequencies due to the reduced period of time that the drive profile is considered. Figure 9 shows the BER and SER of a PLC system transmitted through two Li-ion in series and in parallel when the drive load profile is considered. In comparison with the results that use a static load of  $1 \Omega$ , the difference in results is not immediately apparent. Therefore, the numerical difference in error rates between the static  $1 \Omega$  load and the dynamic drive profile load is shown in Figure 10, whereby it can be seen that only certain carrier frequencies provide substantial improvements in BER of up to 0.15, but only little improvement in SER of up to 0.05 is observed. Noticeable improvements in both BER and SER are observed for cells in series arrangement. The greatest improvement in BER occurred for 64-QAM, but this did not correlate with the same degree of improvement in SER. A greater improvement in BER can be seen for cells in parallel between 10–80 and 160–190 MHz, but only for modulation orders of 16-QAM and above. This improvement in BER did not translate to any change in SER within the same frequency

ranges. This behaviour is due to multiple bits being decoded incorrectly for some symbols when transmitted under the static load model, but not under the dynamic drive load profile due to a favourable reduction in attenuation. Whereas this improves BER, there is no change in SER if there is still one bit set incorrectly within the transmitted symbols. In contrast, a reduction in BER of up to 0.04 for cells in parallel is shown between 90 and 140 MHz, which suggests that a small number of additional bits were changed during transmission at these frequencies, in the opposite effect of that described for the improvements to the BER seen in Figure 10c.

The use of the drive load profile additionally simulates the effects on PLC of a sudden change in drive load, such as through acceleration. These simulations have demonstrated it to be exceptionally rare that corruption of data occurs due to sudden change in drive load. This is because the carrier frequencies tested are orders of magnitude higher than the change in load seen within the drive load profile.

Based upon these comparisons, one can conclude that the most suitable carrier frequency is 30 MHz as previously stated, even when the drive load profile is also considered. First, this frequency has shown to cause stable attenuation and phase shift behaviour from the simulated Li-ion cell configurations. Second, the drive load profile has shown to cause only

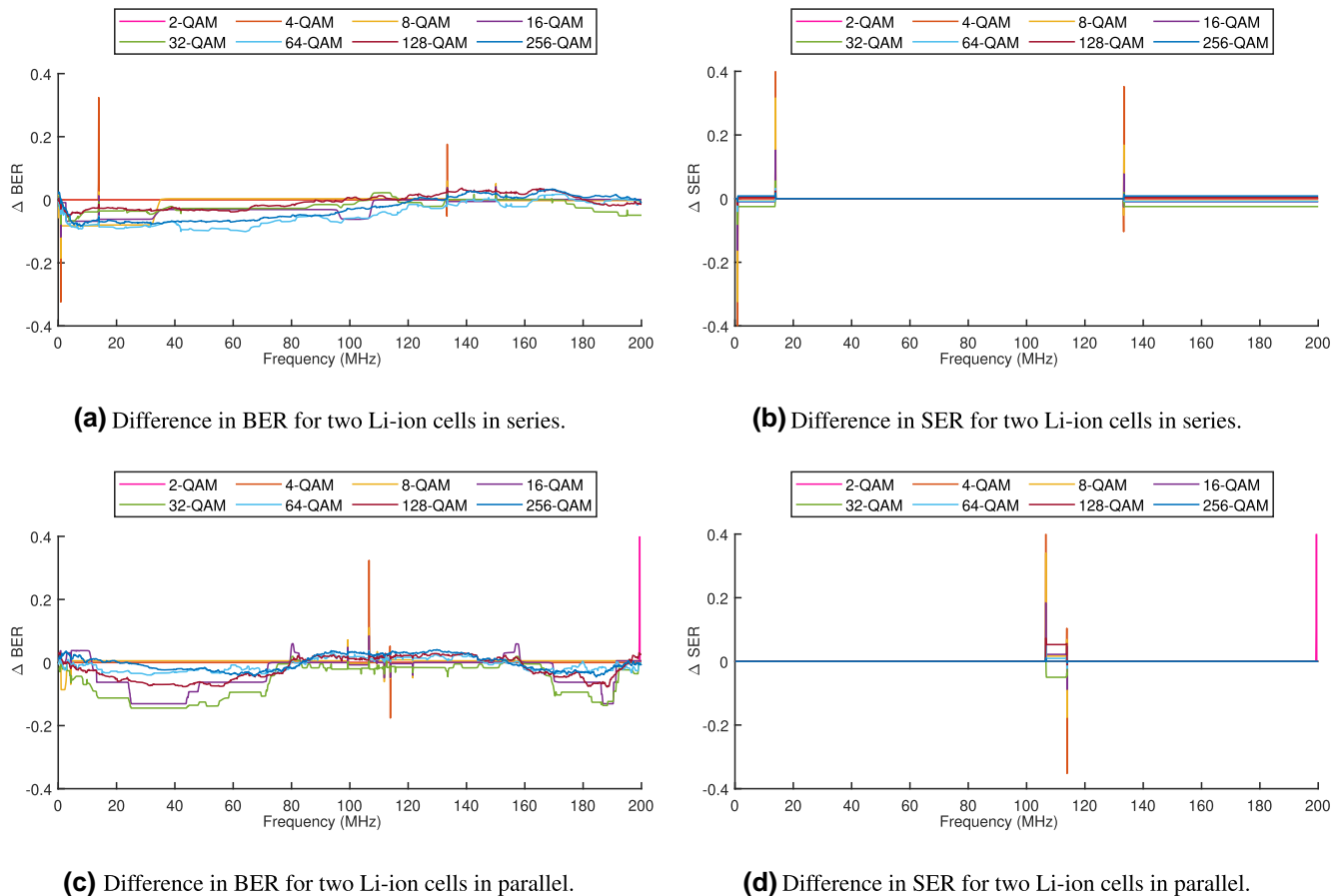


FIGURE 10 Differences in bit and symbol error rates (BER and SER) between a static  $1 \Omega$  load and the dynamic drive profile load

marginal change in error rates at this carrier frequency. This is likely due to the rate of change of the battery load being order of magnitudes lower than that of the carrier frequency.

## 5 | CONCLUSIONS

In this paper, the existing impedance data of both a series and parallel configuration of two in situ connected 18650 cylindrical Li-ion cells were utilised to design a novel battery model to simulate the effects of Li-ion cells on a Power Line Communication (PLC) system that utilises Quadrature Amplitude Modulation (QAM).

Without any analogue filtering or digital error correction, the modelled transmission medium of the two Li-ion cells has been shown to be mostly inadequate for PLC with carrier frequencies between 100 kHz and 200 MHz. This behaviour is due to the significant attenuation of the signal transmitted through the cells when a nominal constant load of  $1 \Omega$  is connected or when real drive profile data is utilised. Furthermore, it has been shown that a parallel arrangement of Li-ion cells results in the highest BER and SER due to the increased magnitude of both attenuation and phase shift in comparison to a series arrangement of cells. However, it has also been concluded that when a carrier frequency of 30 MHz is used, both the attenuation and phase are least frequency dependent, allowing for wider communication channels and increased tolerance for clock jitter. This system requires at least a phase compensation component to counteract the significant (but steady) phase shift observed at that frequency. Moreover, this paper has shown that significant signal amplification will be required for QAM PLC through large BEV battery packs across all evaluated carrier frequencies. A closed-loop amplifier, such as automatic gain control, may be utilised to overcome the observed signal attenuation. Further research is required to ensure that this process does not modify the ASK component of the QAM.

Further research is ongoing to determine how characteristics of individual Li-ion cells scale into large energy storage systems, as well as the effects of SoC and SoH on PLC systems within BEV batteries.

## ACKNOWLEDGEMENTS

This work was supported in part by the UK Engineering and Physical Sciences Research Council (EPSRC) (Grant no. EP/N509796/1 and EP/R513374/1), and in part by the WMG centre High Value Manufacturing Catapult, University of Warwick, Coventry, UK.

The authors would like to thank Dr. Mona Faraji Niri (University of Warwick, Coventry, UK) for kindly providing the raw battery drive profile data used within this research.

## ORCID

Mahyar J. Koshkouei  <https://orcid.org/0000-0002-8643-2909>

Erik Kampert  <https://orcid.org/0000-0002-7159-8578>

## REFERENCES

- Sarmah, S.B., et al.: A review of state of health estimation of energy storage systems: challenges and possible solutions for futuristic applications of li-ion battery packs in electric vehicles. *J. Electrochem. Energy Conv. Storage.* 16(4), (2019)
- Mandal, A.: Greenhouse gas emission from electric vehicle's and Li-ion battery – a review. *Int. J. Mech. Prod. Eng. Res. Dev.* 9(3), 61–74 (2019)
- Zeng, X., et al.: Commercialization of lithium battery technologies for electric vehicles. *Adv. Energy Mater.* 9(27), 1900161 (2019)
- Faraz, A., et al.: Battery electric vehicles (BEVs). In: *Electric Vehicles*, pp. 137–160. Springer Singapore (2020)
- Herrmann, F., Rothfuss, F.: Introduction to hybrid electric vehicles, battery electric vehicles, and off-road electric vehicles. In: *Advances in Battery Technologies for Electric Vehicles*, pp. 3–16. Elsevier (2015)
- Shareef, H., Islam, M.M., Mohamed, A.: A review of the stage-of-the-art charging technologies, placement methodologies, and impacts of electric vehicles. *Renew. Sustain. Energy Rev.* 64, 403–420 (2016)
- Yong, J.Y., et al.: A review on the state-of-the-art technologies of electric vehicle, its impacts and prospects. *Renew. Sustain. Energy Rev.* 49, 365–385 (2015)
- Adhikari, M., et al.: Identification and analysis of barriers against electric vehicle use. *Sustainability.* 12(12), 4850 (2020)
- Andrea, D.: *Battery Management Systems for Large Lithium Battery Packs.* Artech House Publishers (2010)
- Yevgen Barsukov, J.Q.: *Battery Power Management for Portable Devices.* Artech House Publishers (2013)
- Lu, L., et al.: A review on the key issues for lithium-ion battery management in electric vehicles. *J. Power Sources.* 226, 272–288 (2013)
- Tang, X., et al.: A fast estimation algorithm for lithium-ion battery state of health. *J. Power Sources.* 396, 453–458 (2018)
- Li, L.L., Liu, Z.F., Wang, C.H.: The open-circuit voltage characteristic and state of charge estimation for lithium-ion batteries based on an improved estimation algorithm. *J. Test. Eval.* 48(2), 20170558 (2018)
- Attanayaka, A.M.S.M.H.S., Karunadasa, J.P., Hemapala, K.T.M.U.: Estimation of state of charge for lithium-ion batteries – a review. *AIMS Energy.* 7(2), 186–210 (2019)
- Einhorn, M., Roessler, W., Fleig, J.: Improved performance of serially connected Li-ion batteries with active cell balancing in electric vehicles. *IEEE Trans. Veh. Technol.* 60(6), 2448–2457 (2011)
- Gholizadeh, M., Yazdizadeh, A.: Systematic mixed adaptive observer and EKF approach to estimate SOC and SOH of lithium-ion battery. *IET Electr. Syst. Transp.* 10(2), 135–143 (2020)
- Chen, S.X., et al.: Modelling of lithium-ion battery for online energy management systems. *IET Electr. Syst. Transp.* 2(4), 202 (2012)
- Wang, S., et al.: A novel charged state prediction method of the lithium ion battery packs based on the composite equivalent modeling and improved splice Kalman filtering algorithm. *J. Power Sources.* 471, 228450 (2020)
- Fleming, J., et al.: The design and impact of in-situ and operando thermal sensing for smart energy storage. *J. Energy Storage.* 22, 36–43 (2019)
- Ji, F., et al.: Self-reconfiguration batteries with stable voltage during the full cycle without the DC-DC converter. *J. Energy Storage.* 28, 101213 (2020)
- Shang, Y., et al.: A compact resonant switched-capacitor heater for lithium-ion battery self-heating at low temperatures. *IEEE Trans. Power Electron.* 35(7), 7134–7144 (2020)
- Lodi, G.A., et al.: Power line communication in automotive harness on the example of local interconnect network. In: *2016 International Symposium on Power Line Communications and its Applications (ISPLC)*, pp. 212–217. IEEE (2016)
- Talei, A.P., Pribyl, W.A., Hofer, G.: Considerations for a power line communication system for traction batteries. *e & i Elektrotechnik Informationstechnik.* 138(1), 3–14 (2021)
- Ouannes, I., Nickel, P., Dostert, K.: Cell-wise monitoring of lithium-ion batteries for automotive traction applications by using power line communication: battery modeling and channel characterization. In: *18th*

- IEEE International Symposium on Power Line Communications and Its Applications, pp. 24–29. IEEE (2014)
25. Uddin, K., et al.: The effects of high frequency current ripple on electric vehicle battery performance. *Appl. Energy*. 178, 142–154 (2016)
  26. Jiaqi, C., Ruddle, A.R., Teo, Y.X.: Predicting the RF impedance of cells in series for automotive traction battery applications. In: 2017 International Symposium on Electromagnetic Compatibility - EMC EUROPE, pp. 1–6. IEEE (2017)
  27. Teo, Y.X., Chen, J., Ruddle, A.R.: Predicting the RF impedance of cells in parallel for automotive traction battery applications. In: 2019 International Symposium on Electromagnetic Compatibility - EMC EUROPE, pp. 438–443. IEEE (2019)
  28. Zhang, R., et al.: A novel battery management system architecture based on an isolated power/data multiplexing transmission bus. *IEEE Trans. Ind. Electron.* 66(8), 5979–5991 (2019)
  29. Landinger, T.F., et al.: Power line communications in automotive traction batteries: a proof of concept. In: 2020 IEEE International Symposium on Power Line Communications and its Applications (ISPLC), pp. 1–5. IEEE (2020)
  30. Warner, J.T.: *Lithium-Ion Battery Chemistries*. Elsevier (2019)
  31. Jousse, J., et al.: Power line communication management of battery energy storage in a small-scale autonomous photovoltaic system. *IEEE Trans. Smart Grid*. 8(5), 2129–2137 (2017)
  32. Vincent, T.A., Marco, J.: Development of smart battery cell monitoring system and characterization on a small-module through in-vehicle power line communication. *IEEE Access*. 8, 220658–220671 (2020)
  33. Alencar, M.S., da Rocha, V.C.: Quadrature amplitude modulation. In: *Communication Systems*, pp. 157–180. Springer International Publishing (2019)
  34. Andre, D., et al.: Characterization of high-power lithium-ion batteries by electrochemical impedance spectroscopy. i. Experimental investigation. *J. Power Sources*. 196(12), 5334–5341 (2011)
  35. Niri, M.F., et al.: Remaining energy estimation for lithium-ion batteries via Gaussian mixture and markov models for future load prediction. *J. Energy Storage*. 28, 101271 (2020)
  36. Cañete, F.J., et al.: *Power Line Communications*. John Wiley and Sons, Ltd. (2016)

**How to cite this article:** Koshkouei, M.J., et al.: Evaluation of an in situ QAM-based Power Line Communication system for lithium-ion batteries. *IET Electr. Syst. Transp.* 1–11 (2021). <https://doi.org/10.1049/els2.12033>